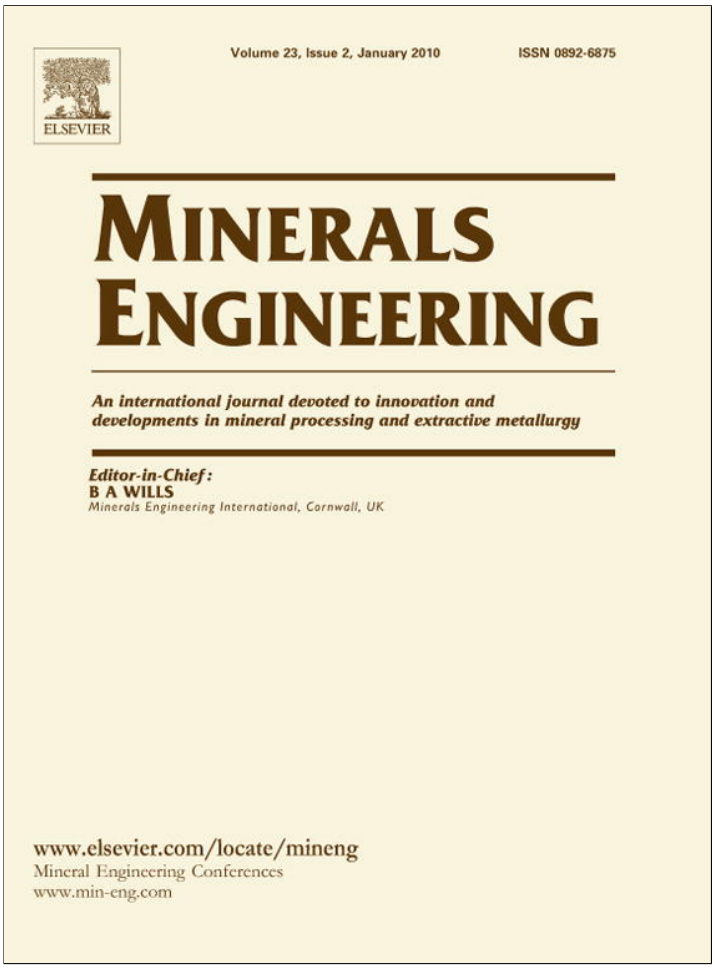

Minerals Engineering 23 (2010) 137–142

Contents lists available at ScienceDirect

Minerals Engineering

journal homepage: www.elsevier.com/locate/mineng

Geometallurgical modelling of the Collahuasi flotation circuit

C.J. Suazo [a,*], W. Kracht [b], O.M. Alruiz [a]

[a] Compañía Minera Doña Inés de Collahuasi, Chile
[b] Mining Engineering Department, Universidad de Chile, Chile

ARTICLE INFO

Article history:
Received 21 September 2009
Accepted 7 November 2009
Available online 1 December 2009

Keywords:
Geometallurgy
Modelling
Flotation kinetics

ABSTRACT

The flotation rate constant was modelled as a function of air dispersion properties and the complete feed particle size distribution by using the collision–attachment–detachment approach and introducing a parameter (Φ) which represents the inherent floatability of the ore. It was found that this parameter Φ is characteristic of the geometallurgical unit and does not depend on the main operating conditions. The parameter Φ is dimensionless and can be estimated either from laboratory testwork or directly from an industrial kinetics survey and can be used to predict industrial operation, provided that the other components of the model are evaluated under actual operation conditions. An empirical expression for the maximum achievable recovery – infinite time recovery – is also presented. The complete model, including flotation rate constant and infinite time recovery, was tested showing good correlation at both laboratory and industrial scale. At industrial scale the model was able to predict metallurgical results in a time frame of several weeks at Compañia Minera Doña Inés de Collahuasi SCM, showing an average relative error of less than 2%.

1. Introduction

Compañía Minera Doña Inés de Collahuasi SCM initiated the development of a new geometallurgical model to characterize its Rosario deposit in terms of its comminution circuit capacity (Alruiz et al., 2009) and flotation performance. The flotation component of the model is now described in detail.

The flotation process is affected, among other factors, by the dispersion of bubbles and particles. The dispersion of gas into bubbles – gas dispersion – has a key impact on the flotation performance, as described in the literature (Schwartz and Alexander, 2006). Gas dispersion in the collection zone can be characterized by several variables, namely, the superficial gas velocity (J_g), the gas holdup (ε_g), the Sauter mean bubble size (d_b), and the bubble surface area flux ($S_b = 6J_g/d_b$) (Nesset et al., 2006). The latter being perhaps the most important gas dispersion property since it represents the flux of available bubble surface for flotation (Gorain et al., 1997, 1998).

Scaling-up laboratory results to industrial scale is a fundamental problem both for designing new operations and for the optimization of existing ones. The similitude approach is usually applied, where similarities between laboratory and industrial conditions are established by using a series of dimensionless parameters such as the Power number, Flux number, and Reynolds number. Another commonly used approach refers to the use of purely empirical correlations (Vallebuona et al., 2003) where regression techniques and statistical analysis of experimental data from laboratory tests are used. Other authors have modelled the flotation rate parameter as a function of operational parameters such as agitation level (rpm), gas flow rate and particle size (Gorain et al., 1997, 1998, 1999; Kracht et al., 2005).

In the current approach, the flotation rate constant for two Collahuasi's geometallurgical units (UGM, from the Spanish "*Unidad GeoMetalurgica*") are modelled as a function of the gas dispersion properties and the flotation feed particle size distribution, along with operational and equipment parameters. The approach has the advantage of allowing the simulation of flotation performance at different scales. The model introduces a dimensionless parameter (Φ), characteristic of the ore type, that can be used to scale-up results from the laboratory to industrial scale.

2. Flotation kinetics modelling in conventional cells

Several authors have modelled flotation as a first order process (Kelsall, 1961; Arbiter and Harris, 1962; Mao and Yoon, 1997), characterized by a flotation rate constant k:

$$\frac{dN_p}{dt} = -kN_p \tag{1}$$

where N_p is the corresponds to the particle concentration in the machine.

Eq. (1) may be written as follows (Sherrell, 2004):

* Corresponding author.
E-mail address: cjsuazo@collahuasi.cl (C.J. Suazo).

0892-6875/$ - see front matter © 2009 Elsevier Ltd. All rights reserved.
doi:10.1016/j.mineng.2009.11.005

$$\frac{dN_p}{dt} = -kN_p = -Z_{pb}P_A(1-P_D)R_f \quad (2)$$

where Z_{pb} is the collision frequency between particles (index p) and bubbles (index b), P_A is the probability of attachment, P_D the probability of detachment and R_f, the froth recovery, which, in the case of low froth depth, tends towards 1 (Gorain et al., 1998). For the purpose of this article, the froth recovery will be assumed to be unity.

From Eq. (2), the flotation rate constant can be written as:

$$k = \frac{Z_{pb}}{N_p}P_A(1-P_D)R_f \quad (3)$$

2.1. Attachment and detachment probability

For flotation modelling, the attachment and detachment processes can be estimated using Eqs. (4) and (5) (Yoon and Lutrell, 1989).

The attachment probability can be estimated as follows:

$$P_A = \text{sen}^2\left[2\cdot\arctan\left(\exp\left(\frac{-(45+8\cdot \text{Re}_b\cdot t_i\cdot U_b)}{15\cdot d_b\cdot(\frac{d_b}{d_p}+1)}\right)\right)\right] \quad (4)$$

where Re_b is the bubble Reynolds number.

The detachment probability, P_D, is given by:

$$P_D = \left(\frac{d_p}{d_{p,\max}}\right)^{1.5} \quad (5)$$

where $d_{p,\max}$ is the maximum floatable particle size fed into the machine, which for this article will be defined as P_{95}, i.e., the particle size under which 95% of the particles can be found.

Eqs. (4) and (5) are empirical formulae, valid for single particle size and do not reflect the behaviour of complete particle size distribution. Therefore, in order to calculate the flotation probabilities described above, two expressions representing weighted average flotation probabilities are introduced:

$$P_A = \sum_{i=1}^{n} P_A^i\cdot f_i, \quad P_D = \sum_{i=1}^{n} P_S^i\cdot f_i \quad (6)$$

where f_i represents the retained fraction in the particle size distribution, and n is the number of fractions in the particle size distribution. This weighted average flotation probabilities allows estimating the effect of the feed particle size distribution on flotation kinetics.

2.2. Bubble size estimation

The bubble size can be estimated using Eq. (7), which is an adaptation (Vallebuona et al., 2003) of Gorain's expression (Gorain et al., 1999):

$$d_b = \frac{6}{a\cdot N_s^b\cdot J_g^{c-1}\cdot \text{As}^d\cdot P_{80}^e} \quad (7)$$

where N_s is the peripheral impeller velocity in (m/s); J_g is the superficial gas velocity (cm/s) and As is the impeller aspect ratio.

Data from survey campaigns with direct measurements of J_g and d_b are necessary to estimate the specific values for the parameters a, b, c, d and e (Gorain et al., 1999; Vallebuona et al., 2003). Although Eq. (7) does not consider frother concentration as a parameter, it works well in cases where the frother dosage is close or beyond the critical coalescence concentration, which is a common practice at industrial scale (Laskowski, 2003).

The model presented in this article considers the Sauter mean bubble size as a single bubble diameter representing the complete bubble size distribution. Further development of this model to include the complete bubble size distribution is under way and will be presented in a future article.

2.3. Collision frequency in turbulent flow

According to Abrahamson's model (Abrahamson, 1975) for turbulent flow, Z_{pb} may be written as follows:

$$Z_{pb} = 2^{2/3}\pi^{1/2}N_pN_b\left(\frac{d_p+d_b}{2}\right)^2\sqrt{\bar{U}_p^2+\bar{U}_b^2} \quad (8)$$

where N_p is the particle concentration expressed as number density and N_b is the number density of bubbles. $\bar{U}_p$ is the particle velocity (Liepe and Moeckel, 1976) and $\bar{U}_b$ is the bubble velocity (Lee and Erickson, 1987), which can be expressed as follows:

$$\sqrt{\bar{U}_p^2} = 0.4\frac{\xi^{4/9}d_p^{7/9}}{\nu^{1/3}}\left(\frac{\rho_s-\rho_l}{\rho_l}\right)^{2/3} \quad (9)$$

$$\bar{U}_b^2 = C_o(\xi d_b)^{2/3} \quad (10)$$

C_o is given by Batchelor (1951) as 2 and ξ corresponds to the energy dissipation rate.

The number density of bubbles (N_b) can be written as a function of gas holdup (ε_g) and bubble size (d_b):

$$N_b = \frac{3\varepsilon_g}{4\pi d_b^3} \quad (11)$$

The gas holdup, on the other hand, can be estimated from the S_b as follows (Finch et al., 2000):

$$\varepsilon_g = \frac{S_b}{5.5} \quad (12)$$

Since none of the expressions used in the model accounts for the inherent floatability of the ore, a dimensionless parameter Φ is included. Therefore, the kinetic rate constant, for turbulent flow conditions, can be expressed as follows:

$$k = \Phi\frac{3\varepsilon_g}{(2\pi)^{1/2}d_p^3}\left(\frac{d_p+d_b}{2}\right)^2\sqrt{\bar{U}_p^2+\bar{U}_b^2}P_A(1-P_D)R_f \quad (13)$$

For simplicity, Eq. (13) may be written as:

$$k = \Phi\cdot F \quad (14)$$

where F corresponds to:

$$F = \frac{3\varepsilon_g}{(2\pi)^{1/2}d_p^3}\left(\frac{d_p+d_b}{2}\right)^2\sqrt{\bar{U}_p^2+\bar{U}_b^2}P_A(1-P_D)R_f \quad (15)$$

Note that F, as expressed in Eq. (15), has units of 1/s and has to be converted to 1/min in order to be used in Eq. (14).

The parameter Φ should not be confused with the parameter P in the $k-S_b$ model proposed by Gorain et al. (1998). In that model, P accounts for the floatability of the ore, and implicitly for everything that S_b does not account for, i.e., probability of attachment, detachment and collision frequency. In the current model, since all those variables are explicitly included in F, the parameter Φ accounts only for the inherent floatability of the ore.

2.4. Scaling-up from laboratory to industrial scale

F takes different values depending on the operating variables, which may differ between laboratory and industrial scale. Therefore, the expression depends on parameters such as impeller size and aspect ratio, together with gas dispersion properties (bubble size and gas holdup). On the other hand, Φ accounts for the inherent floatability of the particles in the collection zone, which means it is unique for a given geometallurgical unit and can be deter-

Table 1
Geometallurgical units defined for Rosario deposit within the period 2008–2012.

UGM	Alteration	Lithology	Proportion by mass (%)
1	Sericite; argillic; chlorite–sericite	Intrusive porphyry	18
2	Sericite; argillic; chlorite–sericite	Hosted rock	26
3	Quartz–sericite; porpylitic; quartz; biotite; potassic	Intrusive porphyry	19
4	Quartz–sericite; porpylitic; quartz; biotite; potassic	Hosted rock	25
5	Sericite; argillic; chlorite–sericite	Intrusive porphyry + hosted rock	7
6	Quartz–sericite; porpylitic; quartz; biotite; potassic	Intrusive porphyry + hosted rock	5

Table 2
Mineralogical composition of UGM1 and UGM5.

Mineral	% Weight	
	UGM1	UGM5
Chalcopyrite	2.10	3.00
Chalcocite	0.18	0.41
Coveline	tr	tr
Enargite	tr	0.16
Bornite	0.48	tr
Soluble Cu	0.07	tr
Cuprite	tr	tr
Sphalerite	tr	tr
Molybdenite	0.15	0.17
Rutile	0.26	0.15
Pyrite	2.39	5.10
Hematite	tr	0.19
Magnetite	0.16	0.37
Limonite	tr	tr
Gangue	94.23	90.46
Total	100	100

Table 3
Operating conditions for laboratory experimental campaign.

Test	P_{80}, μm	Agitation, rpm	J_g, cm/s	N_s, m/s	d_b, mm
1	200	1324	0.97	5.9	2.3
2	250	1324	0.97	5.9	2.6
3	250	1000	0.97	4.5	2.9
4	250	700	0.97	3.1	3.4
5	250	1324	0.70	5.9	2.4
6	250	1324	0.43	5.9	2.1
7	230	1324	0.97	5.9	2.5
8	300	1324	0.97	5.9	2.8
9	560	1324	0.97	5.9	3.6
10	250	1324	0.97	5.9	2.6

Note: Air flow rates reported at 20 psi and 20 °C. Bubble size estimated from Eq. (7).

mined at laboratory scale and used to forecast the flotation kinetics at industrial scale, provided that the system chemistry remains the same (pH, reagent types and dosages). Eq. (14) can be rewritten to yield $K^{\text{INDUSTRIAL}}$, the flotation rate constant at industrial scale, as follows:

$$K^{\text{INDUSTRIAL}} = \Phi \cdot F^{\text{INDUSTRIAL}} \tag{16}$$

Φ in Eq. (16) can be determined at the laboratory, whereas $F^{\text{INDUSTRIAL}}$ is obtained from evaluating Eq. (15) at the industrial operating conditions.

3. Results and discussion

Collahuasi's Rosario deposit is characterized by six geometallurgical units (UGM1–UGM6). The definition of the geometallurgical units was made in two stages, based on previous work developed by the Xstrata Process Support Group, Canada (Fragomeni et al., 2005; Lotter et al., 2002). These stages involved firstly grouping the geometallurgical units on the basis of geological similarities and secondly determining their volumetric fraction in the material that was planned to be processed over the period 2008–2012.

The characteristics of each unit (alteration and lithology), along with the proportion in the deposit, are presented in Table 1.

3.1. Flotation rate constant at laboratory scale

A laboratory flotation test program was carried out using samples of two different geometallurgical units (UGM) from Doña Inés de Collahuasi Mining Company, UGM1 and UGM5, which represent 18% and 7% of the total ore to be processed during the following 3 years, respectively. The mineral was analyzed by microscopy and QEMSCAN, and the composition of both geometallurgical units is presented in Table 2. The average copper grades are 1.12% for UGM1 and 1.37% for UGM5.

The experimental test program carried out with each geometallurgical unit consisted of a series of flotation tests in a Denver lab-

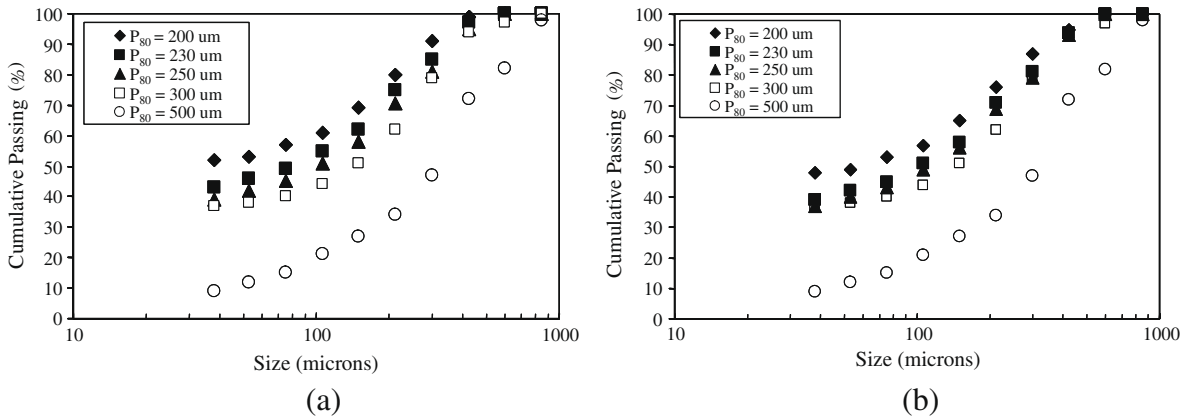

Fig. 1. Particle size distributions at different grinding levels: (a) UGM1 and (b) UGM5.

Table 4
Laboratory rougher kinetics experimental campaign, UGM1.

Test	$\Phi_{UGM-1} = 77 \times 10^{-6}$		
	Klimpel parameters		k Modelled
	$K_{Klimpel}$, min^{-1}	R_∞, %	k_{Model}, min^{-1}
1	4.9	93.9	5.7
2	4.5	89.1	4.1
3	3.2	86.5	2.6
4	1.1	87.0	1.4
5	4.6	89.6	3.7
6	4.0	89.3	2.8
7	4.5	93.1	4.8
8	4.0	83.7	3.4
9	1.8	60.4	1.3
10	4.4	87.4	4.3

Table 5
Laboratory Rougher kinetics experimental campaign, UGM5.

Test	$\Phi_{UGM-5} = 10.2 \times 10^{-5}$		
	Klimpel parameters		k Modelled
	$K_{Klimpel}$, min^{-1}	R_∞, %	k_{Model}, min^{-1}
1	6.6	95.1	7.3
2	5.3	91.8	5.5
3	2.5	88.3	3.3
4	2.1	87.3	1.7
5	5.1	91.5	4.7
6	4.8	92.0	3.7
7	6.3	93.3	6.1
8	4.9	89.5	4.4
9	2.6	78.1	1.7
10	4.3	91.7	5.3

oratory flotation cell modified to receive forced air from an air injection system. The studied variables were the grinding size (P_{80}), agitation (rpm), and gas flow rate (J_g). Ten different combinations of these variables were tested for each geometallurgical unit (see Table 3). The flotation tests were done under conditions as used in Collahuasi concentrator. The collectors used were isopropyl ethyl thionocarbamate and mercaptobenzothiazol (Matcol-123, 25 g/tons; Matcol-154, 19 g/tons), the frothers used were a mix of pine oil, alcohols, ethers and aldehydes (Matfroth-421, 35 g/tons; AX-133, 3 g/tons). Diesel was also added (15 g/tons) and the pH was adjusted to 9.5 with lime. The solids percentage in the tests was 30%.

Table 6
Parameters of Eq. (17) for UGM1 and UGM5.

Parameter	UGM 1	UGM 5
λ_1	0.083	0.028
λ_2	2.96	4.45
λ_3	116.58	109.95
R^2	0.99	0.96

Each P_{80} in Table 3 corresponds to a different particle size distribution (see Fig. 1) and was achieved by varying the grinding time of the ore sample in the laboratory. Especial attention was paid to the grinding process in the laboratory in order to obtain particle size distributions that represented those generated at industrial scale.

For each test, a first order kinetics (Klimpel, 1980) was fitted in order to obtain the experimental flotation rate constant $k_{Klimpel}$. The flotation rate constant for each test was also predicted using the expression proposed in Eq. (13). The value of F (Eq. (15)) was calculated for every test and Φ was determined for both geometallurgical units by minimizing the sum of squared errors between experimental and modelled (predicted) flotation rate constant.

Tables 4 and 5 summarize the experimental results obtained for each geometallurgical unit together with the estimated (modelled) values of the flotation rate constant. The value of Φ is also indicated.

The quality of the prediction can be observed in Fig. 2. The correlation coefficient between the experimental values (the Klimpel fitted flotation rate parameters) and the modelled flotation rate parameters was $R^2 = 0.85$ for both geometallurgical units tested.

3.2. Infinite time recovery

From a statistical analysis of the results, it was found that infinite time recovery is strongly influenced by the bubble size (d_b) and particle size (P_{80}), which allowed the generation of an expression that relates these variables (see Eq. (17)).

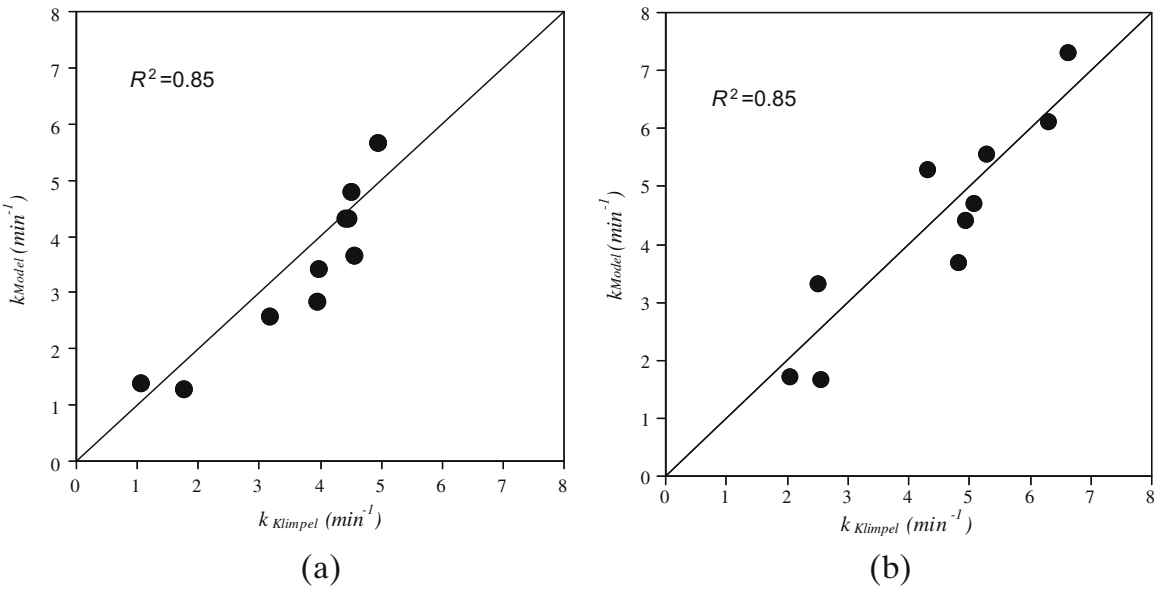

Fig. 2. Experimental rate $k_{Klimpel}$ versus modelled k for UGM1 (a) and UGM5 (b).

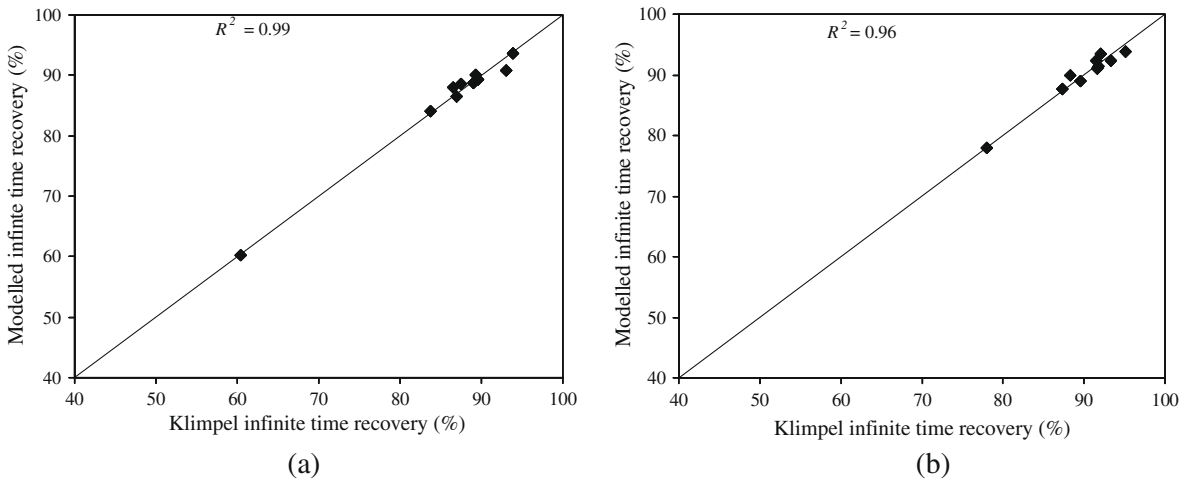

Fig. 3. Infinite time recovery R_∞ for UGM1 (a) and UGM5 (b).

Table 7
Φ Values for each geometallurgical unit.

UGM	$\Phi \times 10^{-5}$
1	7.7
2	8.3
3	13.2
4	7.2
5	10.2
6	11.7

$$R_\infty = -\lambda_1 \cdot P_{80} - \lambda_2 \cdot d_b + \lambda_3 \quad (17)$$

The parameters λ_1, λ_2 and λ_3 in Eq. (17) depend on the ore type (UGM) and system chemistry. Table 6 shows the parameters obtained for each UGM along with the correlation coefficients (R^2). Fig. 3 shows the quality of the fit.

According to Eq. (17), the bubble size (d_b) can be influenced by parameters such us P_{80}, air flow rate, impeller speed and aspect ratio. The same would apply to R_∞, which means that the infinite time recovery depends on the grinding size (P_{80}), as expected, but also depends on the main operating conditions and the impeller design.

3.3. Predicting flotation performance at industrial scale

Each UGM corresponds to a different mineral type, and hence, it has a characteristic Φ value. In order to determine the values of Φ for each geometallurgical unit, the same laboratory work described for UGM1 and UGM5 was repeated. The Φ values are presented in Table 7.

From January 2008 to April 2009, weekly data was collected from the production records. Information included throughput, the P_{80} per grinding line, copper head grade and the particle size distribution fed to the flotation circuit. For each geometallurgical unit, the industrial flotation rate constant was estimated using the Eq. (16). The average agitation level, air flow rate and impeller

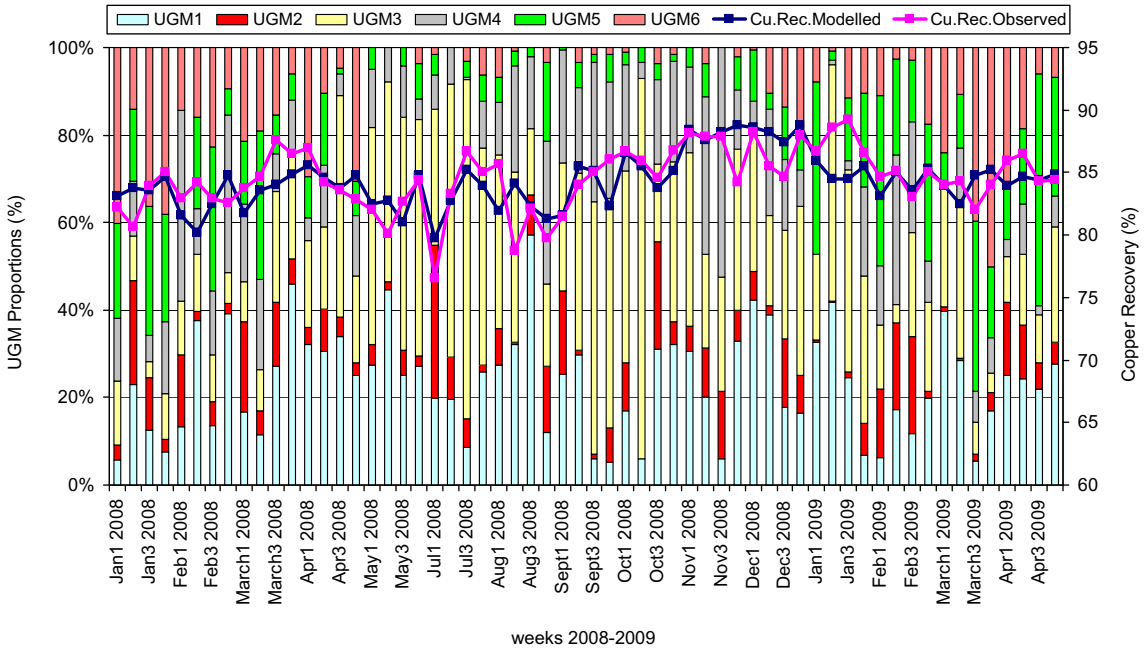

Fig. 4. Comparison between observed and modelled copper recoveries.

Table 8
Prediction of copper recovery using Φ value from industrial survey on Day 1. $\Phi = 7.8 \times 10^{-5}$.

Day	Throughput, tpd	Cu feed grades, %	Cu recovery, %	
			Observed	Modelled
1	123,000	1.10	83.5	83.3
2	131,160	1.21	83.3	83.2
3	121,080	1.12	82.7	82.7
4	122,448	1.19	84.6	84.1
5	125,832	1.15	85.3	85.0
6	126,576	1.17	82.6	82.6

sizes are known for Collahuasi's flotation circuit and for each period or week. The equations presented above were incorporated into a flotation simulator software programmed in Visual C^{++} in order to evaluate the performance of the flotation circuit for different operating conditions.

The proportions of each UGM fed to the plant are known from the mining planning report for the period, which allows estimating the flotation performance with the model presented in this article and comparing it with the actual flotation performance in the plant (from production records). Fig. 4 shows the predictive capacity of the model from January 2008 to April 2009. The proportion of each metallurgical unit fed to the plant is shown for each period.

As it can be seen, the flotation model was able to predict in a satisfactory manner the observed copper recoveries. For each week, the copper recovery for the blend of geometallurgical units was calculated estimating the individual copper recovery for each UGM and then calculating the weighted average using the mass fraction of each UGM in the blend. The calculated average relative error of the model was 1.8%. Note that the good fit of the model supports the assumption of froth recovery equal to 1.

Since each geometallurgical unit has a characteristic Φ, and the model allows scaling-up results between laboratory and industrial scales, the value of Φ could also be determined directly from an industrial kinetic survey and used to model the flotation performance for other days where the same ore (or blend of UGM) is being processed. This was tested at Doña Inés de Collahuasi Mining Company concentrator and the results are presented in Table 8.

After an initial survey performed at the plant (Day 1 in Table 8) to determine the parameter Φ corresponding to the ore being processed, the model was able to predict the recovery of several days of operation at the Doña Inés de Collahuasi Mining Company concentrator. This indicates that the parameter Φ can be obtained either from laboratory tests or from kinetic survey in the actual plant.

4. Conclusions

The results presented in this article show that it is possible to estimate flotation performance in terms of the operating conditions and the complete particle size distribution of the flotation feed. The model considers the probability of flotation and includes a parameter Φ that accounts for the inherent floatability of the mineral.

The parameter Φ is a key component in the model, it is characteristic of the ore type or geometallurgical unit and it does not depend on the scale of the flotation process. Once Φ is determined, it is possible to scale-up the kinetics parameter in order to estimate copper recoveries at industrial scale. This approach was tested with data collected from the production records at Collahuasi's concentrator (from January 2008 to April 2009). The results showed a good prediction of the actual recovery, with an average relative error of 1.8%.

The infinite time recovery R_∞ was empirically modelled as a function of P_{80} and the main operating conditions. The correlation coefficient between experimental and modelled values was over 0.95 for the geometallurgical units studied.

Acknowledgment

The authors would like to thank Doña Inés de Collahuasi Mining Company for its support and the opportunity to write this article.

References

Abrahamson, J., 1975. Collision rates of small particles in a vigorously turbulent fluid. Chemical Engineering Science 30 (11), 1371–1379.
Alruiz, O.M., Morell, S., Suazo, C.J., Naranjo, A., 2009. A novel approach to the geometallurgical modelling of the Collahuasi grinding circuit. Minerals Engineering 22, 1060–1067.
Arbiter, N., Harris, C.C., 1962. In: Fuerstenau, D.W. (Ed.), Flotation Kinetics, Froth Flotation – 50th Anniversary Volume. American Institute of Mining, Metallurgical, and Petroleum Engineers.
Batchelor, G.K., 1951. Pressure fluctuations in isotropic turbulence. In: Proceedings of the Cambridge Philosophical Society, pp. 359–374.
Finch, J.A., Xiao, J., Hardie, C., Gomez, C.O., 2000. Gas dispersion properties: bubble surface area and gas holdup. Minerals Engineering 13 (4), 365–372.
Fragomeni, D., Boyd, L.J., Charland, A., Kormos, L.J., Lotter, N.O., Potts, G., 2005. The use of end-members for grind-recovery modelling, tonnage prediction and flowsheet development at Raglan. In: Canadian Mineral Processor, Ottawa, pp. 75–98.
Gorain, B.K., Franzidis, J.P., Manlapig, E.V., 1997. Studies on impeller type, impeller speed and air flow rate in an industrial cell – Part 4. Effect of bubble surface area flux on flotation performance. Minerals Engineering 10 (4), 367–379.
Gorain, B.K., Franzidis, J.P., Manlapig, E.V., 1998. Studies on impeller type, impeller speed and air flow rate in an industrial cell – Part 5. Validation of k–Sb relationship and effect of froth depth. Minerals Engineering 11 (7), 615–626.
Gorain, B.K., Franzidis, J.P., Manlapig, E.V., 1999. The empirical prediction of bubble surface area flux in mechanical flotation cells from cell design and operating data. Minerals Engineering 12 (3), 309–322.
Kelsall, D.F., 1961. Application of probability in the assessment of flotation systems. Bulletin Institution Mining and Metallurgy 650, 191–204.
Klimpel, R.R., 1980. Selection of chemical reagents for flotation. In: Mular, A., Bhappu, R. (Eds.), Mineral Processing Plant Design. AIME, pp. 907–934.
Kracht, W., Vallebuona, G., Casali, A., 2005. Rate constant modeling for batch flotation, as a function of gas dispersion properties. Minerals Engineering 18 (11), 1067–1076.
Laskowski, J.S., 2003. Fundamental properties of flotation frothers. In: Proceedings of the 22nd International Mineral Processing Congress. Cape Town, South Africa, pp. 788–787.
Lee, C.H., Erickson, L.E., 1987. Bubble breakup and coalescence in turbulent gas–liquid dispersions. Chemical Engineering Communications 59 (1–6), 65–84.
Liepe, F., Moeckel, H.O., 1976. Studies of the combination of substances in liquid phase. Part 6: the influence of the turbulence on the mass transfer of suspended particles. Chemische Technik (Leipzig, Germany) 28 (4), 205–209.
Lotter, N.O., Whittaker, P.J., Kormos, L.J., Stickling, J.S., Wilkie, G.J., 2002. The development of process mineralogy at Falconbridge Limited, and application to the Raglan Mill. CIM Bulletin 95 (1066), 85–92.
Mao, L., Yoon, R.H., 1997. Predicting flotation rates using a rate equation derived from first principles. International Journal of Mineral Processing 51 (1–4), 171–181.
Nesset, J.E., Hernandez-Aguilar, J.R., Acuna, C., Gomez, C.O., Finch, J.A., 2006. Some gas dispersion characteristics of mechanical flotation machines. Minerals Engineering 19 (6–8), 807–815.
Sherrell, I.M., 2004. Development of a Flotation Rate Equation from First Principles Under Turbulent Flow Conditions. Mining and Minerals Engineering. Virginia Polytechnic Institute and State University.
Schwartz, S., Alexander, D., 2006. Gas dispersion measurements in industrial flotation cells. Minerals Engineering 19 (6–8), 554–560.
Vallebuona, G., Suazo, C.J., Casali. A., 2003. Bubble size estimation and rate constant modeling for copper rougher flotation. In: Proceedings of the Copper 2003, vol. 3. Santiago, Chile, pp. 211–224.
Yoon, R.H., Lutrell, G.H., 1989. The effect of bubble size on fine particle flotation. Mineral Processing and Extractive Metallurgy Review 5 (1), 101–102.